ISSN 1063-7834, Physics of the Solid State, 2008, Vol. 50, No. 8, pp. 1401–1406. © Pleiades Publishing, Ltd., 2008.
Original Russian Text © S.G. Ovchinnikov, M.M. Korshunov, E.V. Zakharova, 2008, published in Fizika Tverdogo Tela, 2008, Vol. 50, No. 8, pp. 1349–1354.

METALS
AND SUPERCONDUCTORS

Temperature Evolution of Spin-Polaron In-Gap States in Undoped Antiferromagnetic Cuprates

S. G. Ovchinnikov[a], M. M. Korshunov[a, b], and E. V. Zakharova[a]

[a] *Kirensky Institute of Physics, Siberian Division, Russian Academy of Sciences, Akademgorodok, Krasnoyarsk, 660036 Russia*

e-mail: sgo@iph.krasn.ru, mkor@iph.krasn.ru

[b] *Max-Planck Institut für Physik komplexen Systeme, Dresden, D-01187 Germany*

Received November 7, 2007

Abstract—The temperature evolution of in-gap states created by the spin polaron effect and located within the gap with charge transfer between the valence and conduction bands is studied for the case of strong electron correlations using the t–t'–t''–J model of antiferromagnetic undoped cuprates. The effect of temperature is taken into account by temperature renormalization of the magnon concentration, which is calculated using the Heisenberg model with inclusion of weak interlayer exchange and weak in-plane spin anisotropy, and by introducing a Lorentzian with a temperature-dependent half-width in the form corresponding to the marginal Fermi liquid model. With increasing temperature, the spectral weight of the in-gap state, which is proportional to the magnon concentration, grows leading to an increased intensity of the corresponding peak of the spectral function in all points of the Brillouin zone. At points $(\pi/2, \pi/2)$ and $(\pi, 0)$, the main peak is approached by the satellite peak related to the in-gap band and, at points $(0, 0)$ and (π, π), the peaks move away from each other.

PACS numbers: 74.72.-h, 74.25.Jb, 74.25.Ha, 79.60.-i

DOI: 10.1134/S1063783408080027

1. INTRODUCTION

The key problem in the theory of high-temperature superconductivity (HTSC) is the evolution of the band structure with doping, starting from an antiferromagnetic (AFM) insulator to paramagnet and superconductor. One interesting feature of the electronic structure of the AFM phase of cuprates is the formation of so-called in-gap states located inside the gap with charge transfer between the valence and conduction bands.

The in-gap states in weakly doped cuprates were discovered experimentally [1–3] and found theoretically [4–7] when calculating the properties of small clusters of the t–J model, Hubbard model, and three-band p–d model. Pinning of the chemical potential with increasing doping, which was observed in experiment [8], is also an indirect evidence for in-gap states. Calculations of the band structure of the CuO_2 layer performed within a multiband p–d model [9] in the generalized tight-binding (GTB) approximation [10] with explicit inclusion of strong electron correlations show that an in-gap state in undoped cuprates has a zero spectral weight and that, with increasing doping, it acquires dispersion and a finite spectral weight proportional to the concentration of holes [11, 12].

In all models of strongly correlated systems, the motion of a hole in the presence of AFM ordering is renormalized because of spin fluctuations, which is the essence of the spin-polaron effect. Taking this effect into account in the low-energy model of p-type cuprates, it was concluded in [13] that the interaction between the hole and spin fluctuations is responsible for the formation of an in-gap band. Even in undoped cuprates, such as La_2CuO_4 (LSCO), $Sr_2CuO_2Cl_2$ (SCOC), and $Ca_2CuO_2Cl_2$, (CCOC), in-gap states are manifested as a small low-energy satellite, which can be found in ARPES experiments. It was indicated that points $(\pi, 0)$ and $(\pi/2, \pi/2)$ of the Brillouin zone are the most interesting for experiment, because at these points the satellite peak is at its closest approach to the main spectral peak at the top of the valence band. It was also demonstrated that there are two contributions to the spectral weight of the in-gap band in cuprates, namely, the mean-field contribution, which is proportional to the doping x, and the spin-fluctuation contribution, which is proportional to the magnon concentration $2n(T)$. This concentration depends on temperature, which can lead to a temperature dependence of the satellite spectral peak. The objective of this paper is to investigate the influence of the temperature on the formation of in-gap states in undoped cuprates. The magnon concentration is calculated using the Heisenberg model with inclusion of weak interlayer exchange and weak in-plane spin anisotropy. This model is an effective low-energy model for undoped cuprates.

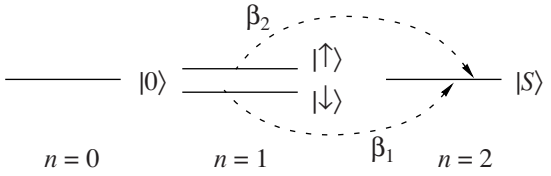

Fig. 1. Hilbert space of the Hubbard model. The dashed arrows indicate quasiparticle excitations in the upper Hubbard band.

2. DISPERSION AND SPECTRAL FUNCTIONS OF IN-GAP STATES

The most general model of layered cuprates is the multiband *p–d* model [9] including not only the $d_{x^2-y^2}$ orbitals of copper and the $p_{x,y}$ orbitals of in-plane oxygen but also the $d_{3z^2-r^2}$ orbitals of copper and the p_z orbitals of apex oxygen. The dispersion laws and spectral densities of quasiparticles and the evolution of the chemical potential with doping calculated within this model in the GTB approximation for both *p*-type [11, 12], and *n*-type [14] compounds are in good agreement with experimental data. The recently developed LDA + GTB method [15] combining ab initio LDA calculations of the parameters of the multiband *p–d* model and the explicit inclusion of strong electron correlations in the GTB approximation made it possible to construct an effective low-energy model for cuprates with parameters obtained from first principles. The *t–t'–t''–J** model (*t–t'–t''–J* model with inclusion of three-center terms) is efficient for *n*-type cuprates and, for *p*-type compounds with a complex structure of the valence band top, the singlet–triplet *t–t'–t''–J** model is appropriate [16].

In this paper, we discuss undoped cuprates and low excitation energies (~2*J*); therefore, the effect of singlet–triplet hybridization on the valence band top is negligibly small. For this reason, we study the spin-polaron effect using the *t–t'–t''–J* model with the Hamiltonian

$$H_{t-J} = (\varepsilon_1 - \mu)\sum_{f,\sigma} X_f^{\sigma\sigma} + \sum_{f\neq g,\sigma} t_{fg} X_f^{\sigma 0} X_g^{0\sigma} + \sum_{f\neq g} J_{fg}\left(\mathbf{S}_f\mathbf{S}_g - \frac{1}{4}n_f n_g\right).$$

Here, t_{fg} is the hopping integral between sites f and g, J_{fg} is the exchange integral, $X_f^{pq} = |p_f\rangle\langle q_f|$ is a Hubbard operator ($|p_f\rangle$ and $|q_f\rangle$ are states at site f), $\mathbf{S}_f$ is the spin operator, n_f is the particle number operator, and $(\varepsilon_1 - \mu)$ is the difference between the single-electron energy and the chemical potential.

The spin and particle number operators can be expressed in terms of Hubbard *X* operators as follows:

$$S_f^+ = X_f^{\sigma\bar{\sigma}}, \quad S_f^- = X_f^{\bar{\sigma}\sigma},$$

$$S_f^z = \frac{1}{2}(X_f^{\sigma\sigma} - X_f^{\bar{\sigma}\bar{\sigma}}), \quad n_{f\sigma} = \sum_{\sigma} X_f^{\sigma\sigma}.$$

In the GTB approximation, an electron in a strongly correlated system is described as a superposition of quasiparticles related to excitations between multielectron *n*- and (*n* + 1)-hole terms of the unit cell, which is taken to be the CuO_6 cluster. Figure 1 shows two quasiparticles, β_1 and β_2, forming the top of the valence band in the AFM phase (in the paramagnetic phase, the spin-up and spin-down levels in the single-hole sector are degenerate and, therefore, only one type of quasiparticles $\beta_1 = \beta_2$ exists). The spectral weight of these quasiparticles in the mean field approximation is determined by the filing of the initial and final states, i.e., by the filling factors of single-particle states $n_{A\sigma}$ and $n_{B\sigma}$, where *A* and *B* enumerate the AFM sublattices and n_S are the filling factors of the lowest two-particle state (singlet $|S\rangle$ of $^1A_{1g}$ symmetry). The filling factors $n_m = \langle X^{mm}\rangle$ are calculated self-consistently using the equation for the chemical potential. In the Hubbard-I approximation, for the hole concentration $n_h = 1 + x$ at a zero temperature, we have $n_{A\uparrow} = n_{B\downarrow} = (1 - x)$, $n_{A\downarrow} = n_{B\uparrow} = 0$, and $n_S = x$. Therefore, the spectral weights of the quasiparticles on the *A* sublattice are

$$F_A(\beta_1) = n_S + n_{A\uparrow} = 1, \quad F_A(\beta_2) = n_S + n_{A\downarrow} = x.$$

It follows that it is β_2 that forms the doping-dependent in-gap band.

In order to go beyond the Hubbard-I approximation, it is necessary to calculate one-loop corrections to the self-energy [17]. In the ferromagnetic and AFM states, the main contribution at low temperatures $T \ll J$ comes from spin-wave excitations (the spin-polaron effect) [18]. According to [18], the main effect of spin excitations is the spin-wave renormalization of the filling factors:

$$\begin{aligned} n_{A\uparrow} &= (1-x)(1-n_{sf}), \\ n_{A\downarrow} &= (1-x)n_{sf}, \quad n_S = x. \end{aligned} \tag{1}$$

Here, $n_{sf} = n(T) - n(0)$, where $n(0)$ and $n(T)$ are the magnon concentrations at zero and finite temperatures, respectively. Generally, n_{sf} is related to the decrease in the sublattice magnetization due to spin fluctuations

$$\langle S_A^z\rangle = (1-x)[1/2 - (n(0) + n_{sf})]. \tag{2}$$

With Eq. (2), the spectral weights of quasiparticles on the *A* sublattice are given by

$$F_A(\beta_1) = x + (1-x)(1-n_{sf}),$$

$$F_A(\beta_2) = x + (1-x)n_{sf}.$$

For small values of x and n_{sf}, we have $F_A(\beta_1) \approx 1 - n_{sf}$ and $F_A(\beta_2) \approx x + n_{sf}$.

So, even at $x = 0$ ($T \neq 0$), we get $F_A(\beta_2) \neq 0$; i.e., the spin-polaron effect should lead to the formation of in-gap states even in undoped $Sr_2CuO_2Cl_2$ and La_2CuO_4 compounds at a nonzero temperature.

We decouple the equations of motion for the electron Green's function $\hat{G}_{k\sigma}$ for the t–t'–t''–J model in the Hubbard-I approximation but take into account the renormalization of the filling factors given by Eq. (1), which corresponds to taking into account the main contributions to the self-energy operator at low temperatures [18]. As a result, we find the energy spectrum of quasiparticles to be

$$E^{\pm}_{k\uparrow} = \varepsilon_1 - \mu + \frac{1}{2}[t^A_k + t^{A'}_k - J^B_0 - J^A_0 - J^{A'}_0 \pm K_k], \quad (3)$$

where

$$K_k = \sqrt{(t^A_k + t^{A'}_k - J^B_0 + J^A_0 + J^{A'}_0)^2(1-2n_{sf})^2 + 4(t^B_k)^2(1-n_{sf})n_{sf}};$$

t^B_k and J^B_0 are the hopping and exchange integrals in momentum space, respectively, between nearest neighbors; and t^A_k and $t^{A'}_k$ (J^A_0 and $J^{A'}_0$) are the hopping (exchange) integrals between second and third nearest neighbors, respectively.

The spectral functions $A_{k\sigma}(E) = -\frac{1}{\pi}\mathrm{Im}[\mathrm{Tr}\,\hat{G}_{k\sigma}]$ can be written as

$$\begin{aligned} A_{k\uparrow}(E) &= u^2_k\delta(E - E^+_{k\uparrow}) + v^2_k\delta(E - E^-_{k\uparrow}), \\ A_{k\downarrow}(E) &= v^2_k\delta(E - E^+_{k\downarrow}) + u^2_k\delta(E - E^-_{k\downarrow}), \end{aligned} \quad (4)$$

where

$$u^2_k = \frac{1}{2} - (1-2n_{sf})^2\frac{(J^B_0 - J^A_0 - J^{A'}_0 - t^A_k - t^{A'}_k)}{2\Delta E_k},$$

$$v^2_k = 1 - u^2_k, \quad \Delta E_k \equiv E^+_{k\uparrow} - E^-_{k\uparrow}.$$

Taking into account the hopping integrals to third nearest neighbors, we get

$$t^B_k = 2t(\cos k_x + \cos k_y), \quad t^A_k = 4t'\cos k_x \cos k_y,$$

$$t^{A'}_k = 2t''(\cos 2k_x + \cos 2k_y),$$

$$J^B_0 = 4J, \quad J^A_0 = 4J', \quad J^{A'}_0 = 4J''.$$

If n_{sf} is zero, we immediately get one dispersion-free state and one state with dispersion (which is determined by intrasublattice hopping integrals t' and t'')

$$\begin{aligned} E^-_{k\uparrow}\big|_{n_{sf}=0} &= \varepsilon_1 - \mu - J^A_0 - J^{A'}_0, \\ E^+_{k\uparrow}\big|_{m_{sf}=0} &= \varepsilon_1 - \mu + t^A_k + t^{A'}_k - J^B_0. \end{aligned} \quad (5)$$

For $n_{sf} = 0$, we have $u^2_k = 0$, $v^2_k = 1$, and only one nonzero spectral function $A_{k\uparrow}(E) = \delta(E - E^-_{k\uparrow})$ remains corresponding to the valence band top for p-type cuprates (the state with dispersion given by Eq. (5)).

Since the hopping and exchange parameters in the t–t'–t''–J model are obtained using the LDA + GTB method [15], the only unknown parameter of the problem is the magnon concentration $n(T)$. In the next section, we calculate this parameter or, more precisely, the sublattice magnetization (2).

3. TEMPERATURE DEPENDENCE OF SPECTRAL FUNCTIONS

As noted in the previous section, the spectral weight of quasiparticles is proportional to the magnon concentration. Therefore, the evolution of the spectral functions with temperature is mainly determined by the temperature dependence of this concentration. Earlier, when analyzing neutron diffraction experiments, we estimated the magnon concentration to be $n(0) \approx 0.138$ [13]. However, this estimate is insufficient for finding the temperature dependence of the spectral peaks. Undoped cuprates are AFM insulators. Therefore, we employ the quasi-two-dimensional Heisenberg model for spin 1/2 in order to describe the spin subsystem and calculate the temperature dependence of the magnon concentration. In [19], it was demonstrated that, in this model, weak in-plane spin anisotropy η has a significant effect on the Néel temperature. Therefore, we also investigate the influence of this parameter on the temperature dependence of n_{sf}.

We write the Hamiltonian of the Heisenberg model in the form

$$\hat{H} = J\Bigg(\sum_{i,\delta_1}\mathbf{S}_i\mathbf{S}_{i+\delta_1} + \eta\sum_{i,\delta_1}S^z_iS^z_{i+\delta_1} + \lambda_2\sum_{i,\delta_2}\mathbf{S}_i\mathbf{S}_{i+\delta_2} + \lambda_3\sum_{i,\delta_3}\mathbf{S}_i\mathbf{S}_{i+\delta_3} + \sum_{i,\delta_{\perp_j}}\lambda_\perp\mathbf{S}_i\mathbf{S}_{i+\delta_{\perp_j}}\Bigg),$$

where J is the nearest neighbor exchange interaction; λ_2 and λ_3 ($\lambda_i = J_i/J$, where $i = 2, 3$) describe in-plane exchanges between the second and third nearest neighbors, respectively; η is the in-plane spin anisotropy; and $\lambda_{\perp_j}$ describe interlayer exchanges. In the undoped state, the low-temperature phase of La_2CuO_4 is orthorhombic, but the crystal structure of La_2CuO_4 becomes tetragonal with doping (so-called T structure). This structure is typical of the superconducting phase. For this reason, the tetragonal structure was discussed in many papers even when studying undoped LSCO. The validity of this approach was illustrated in [19]. We also deal with the tetragonal structure of LSCO.

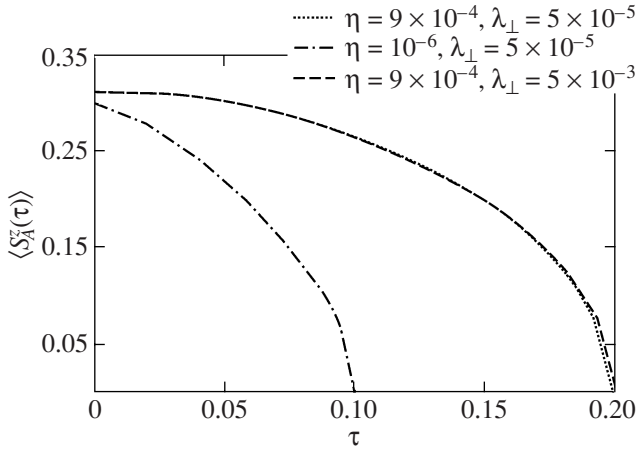

Fig. 2. Temperature dependence of the sublattice magnetization for three different sets of parameters η and $\lambda_\perp$ (J = 0.141 eV, $\lambda_2 = \lambda_3 = 0.0942$ [19]). The temperature scale is given in dimensionless units ($\tau = T/J$).

The exact equation of motion for S_l^+ can be linearized using the Tyablikov approximation [20]

$$i\dot{S}_l^+ = 2J\Bigg(\sum_{\delta_1}\langle S_l^z\rangle S_{l+\delta_1}^+ - (1+\eta)\sum_{\delta_1}\langle S_{l+\delta_1}^z\rangle S_l^+$$
$$+\lambda_2\sum_{\delta_2}\langle S_l^z\rangle S_{l+\delta_2}^+ - \lambda_2\sum_{\delta_2}\langle S_{l+\delta_2}^z\rangle S_l^+$$
$$+\lambda_3\sum_{\delta_3}\langle S_l^z\rangle S_{l+\delta_3}^+ - \lambda_3\sum_{\delta_3}\langle S_{l+\delta_3}^z\rangle S_l^+$$
$$+\lambda_\perp\sum_{\delta_\perp^{\mathrm{FM}}}\langle S_l^z\rangle S_{l+\delta_\perp^{\mathrm{FM}}}^+ - \lambda_\perp\sum_{\delta_\perp^{\mathrm{FM}}}\langle S_{l+\delta_\perp^{\mathrm{FM}}}^z\rangle S_l^+$$
$$+\lambda_\perp\sum_{\delta_\perp^{\mathrm{AFM}}}\langle S_l^z\rangle S_{l+\delta_\perp^{\mathrm{AFM}}}^+ - \lambda_\perp\sum_{\delta_\perp^{\mathrm{AFM}}}\langle S_{l+\delta_\perp^{\mathrm{AFM}}}^z\rangle S_l^+\Bigg).$$

To calculate thermodynamic properties, we use the two-time retarded commutator Green's functions at finite temperatures ($f \in A$, $g \in B$, where A and B specify the magnetic sublattices)

$$\langle\langle S_f^+|S_{f'}^-\rangle\rangle_E = \frac{2}{N}\sum_k G_k^{AA}(E)e^{ik(f-f')},$$

$$\langle\langle S_g^+|S_{f'}^-\rangle\rangle_E = \frac{2}{N}\sum_k G_k^{BA}(E)e^{ik(g-f')}.$$

In the momentum representation, the Green's functions can be found to be

$$G_k^{AA}(E) = \frac{2S(E+Sn(k))}{E^2 - S^2(n^2(k) - I^2(k))} \equiv \frac{2S(E+Sn(k))}{E^2 - S^2E^2(k)},$$

$$G_k^{BB}(E) = \frac{2S(E-Sn(k))}{E^2 - S^2(n^2(k) - I^2(k))} \equiv \frac{2S(E-Sn(k))}{E^2 - S^2E^2(k)},$$

$$G_k^{AB} = G_k^{BA}(E) = -\frac{2S^2I(k)}{E^2 - S^2(n^2(k) - I^2(k))}$$
$$\equiv -\frac{2S^2I(k)}{E^2 - S^2E^2(k)},$$

where

$$n(k) = 2J\Bigg[(1-\eta)z_1 + \frac{z_\perp}{2}\lambda_\perp - \lambda_2 z_2(1 - \cos k_x\cos k_y)$$
$$-\lambda_3 z_3\Bigg(1 - \frac{\cos 2k_x + \cos 2k_y}{2}\Bigg)$$
$$-\frac{z_\perp\lambda_\perp}{2}\Bigg(1 - \cos\frac{(k_x - k_y)}{2}\cos\frac{k_z}{2}\Bigg)\Bigg],$$

$$I(k) = 2J\Bigg[\frac{z_1}{2}(\cos k_x + \cos k_y)$$
$$+\frac{z_\perp\lambda_\perp}{2}\cos\frac{(k_x + k_y)}{2}\cos\frac{k_z}{2}\Bigg].$$

Here, z_i (i = 1, 2, 3, $\perp$) is the number of corresponding neighbors. Therefore, for S = 1/2, the self-consistent equation for the AFM order parameter $S(\tau)$ ($\tau = T/J$ is the dimensionless temperature) can be written as

$$S(\tau) = \frac{1/2}{I(\tau)}, \quad I(\tau) = \frac{2}{N}\sum_k \frac{n(k)}{E(k)}\coth\frac{S(\tau)E(k)}{2\tau}. \quad (6)$$

For $\tau \longrightarrow 0$ ($\coth x \longrightarrow 1$), we obtain the magnetization at a zero temperature to be

$$S(0) = \frac{1/2}{I_1}, \quad I_1 = \frac{2}{N}\sum_k \frac{n(k)}{E(k)}.$$

In the opposite limit $\tau \longrightarrow \tau_N$ (τ_N is the Néel temperature), we have $S(\tau) \longrightarrow 0$. Since $\coth(x) \longrightarrow 1/x$ as $x \longrightarrow 0$, the critical temperature can be found from Eq. (6) to be

$$\tau_N = \frac{1/4}{I_2}, \quad I_2 = \frac{2}{N}\sum_k \frac{n(k)}{E^2(k)}.$$

Figure 2 shows the temperature dependence of the sublattice magnetization for three different sets of parameters η and $\lambda_\perp$ (J = 0.141 eV, $\lambda_2 = \lambda_3 = 0.0942$ [19]). It is seen that the influence of the in-plane anisot-

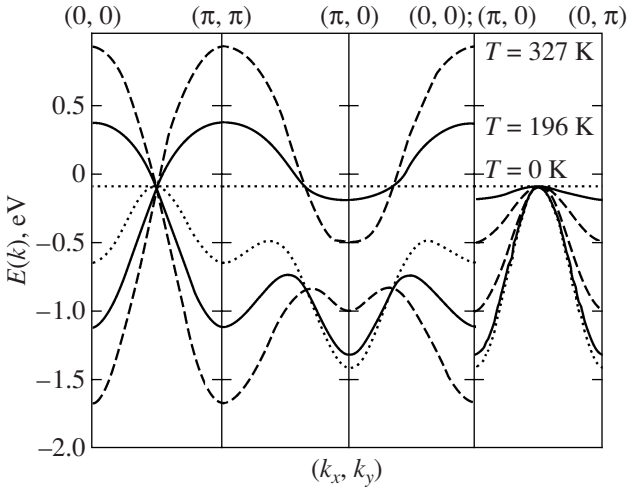

Fig. 3. Dispersion of quasiparticles along the main directions in the Brillouin zone of a square lattice at various temperatures: $T_1 = 0$ K (dotted line), $T_2 = 196$ K (solid line), and $T_3 = 327$ K (dashed line).

ropy η on the magnetization is much stronger than that of the interlayer exchange. An increased anisotropy stabilizes the AFM order, and the Néel temperature increases. The best fit to the experimental value of the Néel temperature $T_N = 325 \pm 5$ K [21–23] is achieved with the following parameter values: $\eta = 9 \times 10^{-4}$ and $\lambda_\perp = 5 \times 10^{-5}$. We use them in the calculations below. With these values, the magnetization at a zero temperature is $S(0) = 0.3119$.

Figure 3 shows quasiparticle dispersion curves for various temperatures: $T_1 = 0$ K, $T_2 = 196$ K, and $T_3 = 327$ K. The parameters of the t–t'–J model for p-type cuprates are taken from [15, Table IV] and they are as follows: $t = 0.679$ eV, $t' = -0.093$ eV, $J = 0.141$ eV, and $J' = J'' = 0.013$ eV. It can be seen in Fig. 3 that the distance between the two branches of the quasiparticle spectrum at points (π, 0) and (π/2, π/2) decreases with increasing temperature.

Figure 4 shows the temperature dependences of the spectral functions at several symmetry points of the Brillouin zone. The employed approximation provides no information about the width of the spectral lines, because the expressions for the spectral functions contain simple delta functions. We artificially widened the spectral peaks using a Lorentzian with a half-width $\delta = \sqrt{E^2 + \pi^2 T^2}$ (which corresponds to the non-Fermi-liquid approach) and set $E = 0.02$ eV, which is equal to the experimental resolution of ARPES measurements. In addition to the main spectral peak, a small satellite appears at an energy above –0.5 eV for nonzero values of n_{sf}. This satellite peak is the in-gap state due to the spin-polaron effect, and its spectral weight is proportional to $n_{sf}(T)$. With increasing temperature, the spectral weight of the in-gap state, which is proportional to $n_{sf}(T)$, increases, leading to an increased intensity of the

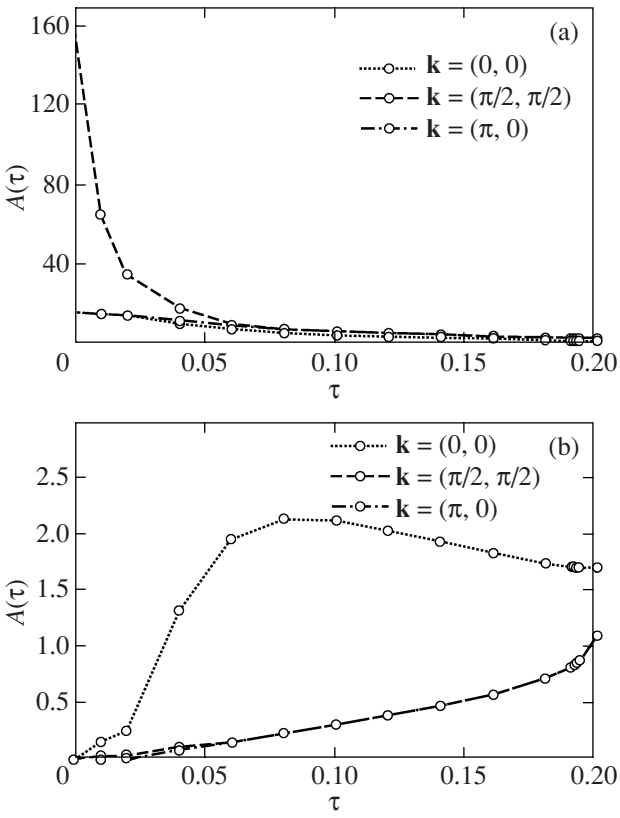

Fig. 4. Dependence of the spectral functions on temperature ($\tau = T/J$) at three symmetry points of the Brillouin zone: (a) the amplitudes of the main peaks and (b) the amplitudes of the in-gap satellites.

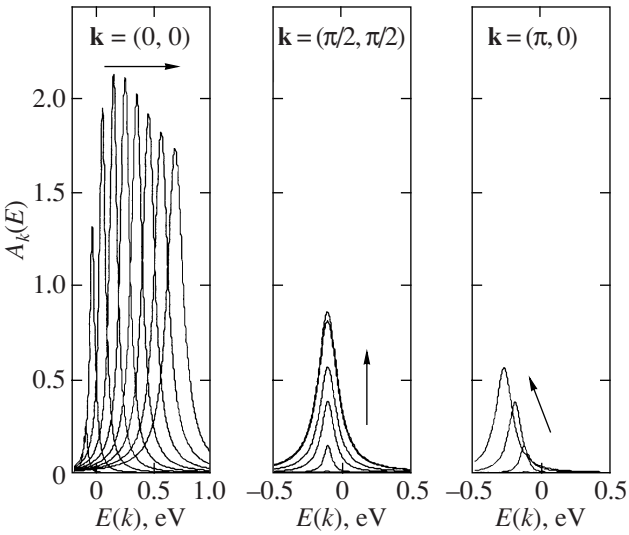

Fig. 5. Variation of the spectral functions of the in-gap satellites with dimensionless temperature τ at three symmetry points of the Brillouin zone. Arrows indicate the direction of an increase in temperature.

corresponding spectral peak at all points of the Brillouin zone. This pattern is in qualitative agreement with the results from [26], where analogous calculations were performed within the t–t'–t''–J model by exact diagonalization.

4. CONCLUSIONS

In this paper, we have taken into account the effect of temperature through renormalization of the magnon concentration, which has been calculated using the Heisenberg model with inclusion of the weak interlayer exchange and weak in-plane spin anisotropy. Because of strong correlations, the renormalizations of the filling factors not only vary the intensities of peaks in the spectral functions but also change their positions; i.e., they modify the momentum dependence of the quasiparticle spectrum. As a result, both the relative energy positions of the peaks (Fig. 5) and their intensities vary with increasing temperature. The largest displacements of the satellite peaks take place at point (0, 0). However, because the matrix element of photoelectron excitation is small near the Γ point, these changes cannot be detected in ARPES experiments. Therefore, we propose studying the increase in the intensity of the satellites at points $(\pi, 0)$ and $(\pi/2, \pi/2)$ indicated in Fig. 5 by arrows, which is possible with the ARPES method.

The effects of the finite quasiparticle lifetime due to scattering on thermal and spin fluctuations have been modeled by introducing a finite-width Lorentzian instead of the delta functions in Eq. (4). This approach does not account for the strong k dependence of damping of the quasiparticles, which can cause substantial smearing of the spectral peaks at certain k points and make their observation impossible. However, as demonstrated in this study, the intensity of the satellite spectral peak at room temperature is nonzero for any momentum. Therefore, strong suppression of the peak intensity at certain k points does not preclude observations of the in-gap state.

ACKNOWLEDGMENTS

This work was supported by the Russian Foundation for Basic Research (project nos. 06-02-16100 and 06-02-90537-BNTS), the Presidium of the Russian Academy of Sciences (program "Quantum Macrophysics"), and INTAS (YS grant no. 05-109-4891).

REFERENCES

1. M. Suzuki, Phys. Rev. B: Condens. Matter **39**, 2312 (1989).
2. S. Uchida, T. Ido, H. Takagi, T. Arima, Y. Tokura, and S. Tajima, Phys. Rev. B: Condens. Matter **43**, 7942 (1991).
3. A. V. Bazhenov, A. V. Gorbunov, and V. E. Timofeev, Zh. Éksp. Teor. Fiz. **104** (3), 3193 (1993) [JETP **77** (3), 500 (1993)].
4. W. Stephan and P. Horsch, Phys. Rev. Lett. **66**, 2258 (1991).
5. E. Dagotto, A. Moreo, F. Ortolani, J. Riera, and D. J. Scalapino, Phys. Rev. Lett. **67**, 1918 (1991).
6. Y. Ohta, K. Tsutsui, W. Koshibae, T. Shimozato, and S. Maekawa, Phys. Rev. B: Condens. Matter **46**, 14 022 (1992).
7. R. Press, W. Hanke, and W. von der Linden, Phys. Rev. Lett. **75**, 1344 (1995).
8. N. Harima, J. Matsuno, A. Fujimori, Y. Onose, Y. Taguchi, and Y. Tokura, Phys. Rev. B: Condens. Matter **64**, 220 507R (2001).
9. Yu. Gaididei and V. Loktev, Phys. Status Solidi B **147**, 307 (1988).
10. S. G. Ovchinnikov and I. S. Sandalov, Physica C (Amsterdam) **161**, 607 (1989).
11. V. A. Gavrichkov, S. G. Ovchinnikov, A. A. Borisov, and E. G. Goryachev, Zh. Éksp. Teor. Fiz. **118** (2), 422 (2000) [JETP **91** (2), 369 (2000)].
12. V. Gavrichkov, A. Borisov, and S. G. Ovchinnikov, Phys. Rev. B: Condens. Matter **64**, 235 124 (2001).
13. S. G. Ovchinnikov, A. A. Borisov, V. A. Gavrichkov, and M. M. Korshunov, J. Phys.: Condens. Mater **16**, L93 (2004).
14. V. A. Gavrichkov and S. G. Ovchinnikov, Zh. Éksp. Teor. Fiz. **125** (3), 630 (2004) [JETP **98** (3), 556 (2004)].
15. M. M. Korshunov, V. A. Gavrichkov, S. G. Ovchinnikov, I. A. Nekrasov, Z. V. Pchelkina, and V. I. Anisimov, Phys. Rev. B: Condens. Matter **72**, 165 104 (2005).
16. M. M. Korshunov and S. G. Ovchinnikov, Fiz. Tverd. Tela (St. Petersburg) **43** (3), 399 (2001) [Phys. Solid State **43** (3), 416 (2001)].
17. R. O. Zaĭtsev, Zh. Éksp. Teor. Fiz. **68** (1), 207 (1975) [Sov. Phys. JETP **41** (1), 100 (1975)].
18. A. N. Podmarkov and I. S. Sandalov, Zh. Éksp. Teor. Fiz. **86** (4), 1461 (1984) [Sov. Phys. JETP **59** (4), 856 (1984)].
19. M. Manojlović, M. Pavkov, M. Škrinjar, M. Pantić, D. Kapor, and S. Stojanović, Phys. Rev. B: Condens. Matter **68**, 014 435 (2003).
20. S. V. Tyablikov, *Method in the Quantum Theory of Magnetism*, 2nd ed. (Plenum, New York, 1967; Nauka, Moscow, 1975).
21. R. J. Brigeneau, M. Greven, M. A. Kaster, Y. S. Lee, B. O. Wells, and G. Shirane, cond-mat/9903124.
22. J. Rossat-Mignod, L. P. Regnault, P. Bourges, P. Burlet, C. Vettier, and J. Y. Henry, *Frontiers in Solid State Sciences: Magnetism and Superconductivity* (Word Sci., Singapore, 1994).
23. B. Keimer, N. Belk, R. J. Brigeneau, A. Cassanho, C. Y. Chen, R. W. Irwin, and G. Shinare, Phys. Rev. B: Condens. Matter **46**, 14 034 (1992).
24. C. M. Varma, P. B. Littlewood, and S. Schmitt-Rink, Phys. Rev. Lett. **63**, 1996 (1989).
25. M. M. Zemljic and P. Prelovsek, Phys. Rev. B: Condens. Matter **75**, 104 514 (2007).
26. Y. Shibata, T. Tohyama, and S. Maekawa, Phys. Rev. B: Condens. Matter **59**, 1840 (1999).

Translated by G. Tsydynzhapov